Construction of an Improved Tandem Time-of-flight Mass Spectrometer for Photodissociation of Ions Generated by Matrix-assisted Laser Desorption Ionization (MALDI)

Jeong Hee Moon, So Hee Yoon, and Myung Soo Kim*

*National Creative Research Initiative Center for Control of Reaction Dynamics and School of Chemistry, Seoul National University, Seoul 151-742, Korea. *E-mail: myungsoo@plaza.snu.ac.kr*
Received February 23, 2005

An improved tandem time-of-flight (TOF) mass spectrometer for the photodissociation (PD) study of ions generated by matrix-assisted laser desorption ionization (MALDI), MALDI-TOF-PD-TOF, has been designed and constructed. Recording a full spectrum with better than unit mass resolution even in low mass range has been achieved without reflectron voltage stepping which was needed in the previous version. Other aspects of the improvement, such as those in the data system which now allow 10-100 times faster spectral acquisition than with the previous instrument, are described. Rationale for the ideas which have led to the improvements is presented also.

Key Words : MALDI, Tandem mass spectrometry, MALDI-TOF-PD-TOF

Introduction

Matrix-assisted laser desorption ionization (MALDI)[1,2] is a useful method to generate ions from samples in condensed phase. Since MALDI is a pulsed ionization technique, it is advantageous to use a time-of-flight (TOF) spectrometer to record the mass spectrum. MALDI-TOF is widely used to obtain mass spectra of various biological molecules such as proteins, peptides, nucleic acids, etc. and to determine their relative molecular masses.

Tandem mass spectrometry, which analyzes daughter ions generated from a mass-selected parent ion, is often performed to gain further structural information. There are several ion activation methods to induce fragmentation of a parent ion. The simplest among these is the post-source decay (PSD)[3,4] which records spontaneous unimolecular reactions of a parent ion. The internal energy of the parent ion gained in the source is the driving force for these reactions. When neutral gas is introduced onto the ion flight path, collision activation of the parent ion can occur. Recording the daughter ions generated *via* collisionally activated dissociation (CAD)[2] is another useful method to obtain tandem TOF mass spectra.

The internal energy of a parent ion can be increased by photoabsorption also.[5-8] In fact, photodissociation (PD) has been used for the fundamental studies on ion structure and dissociation dynamics.[9] Recently, we reported the design and construction of a photodissociation tandem TOF mass spectrometer equipped with a MALDI source, or MALDI-TOF-PD-TOF.[10] It was demonstrated that substantial fractions of protonated peptides could be photodissociated at 266 nm. Even complete depletion was possible as the PD laser intensity was increased. Also, the PD spectra were found to contain rich structural information relevant to the peptide sequence determination.[11]

The second stage analyzer of conventional tandem TOF mass spectrometers is usually a constant field reflectron.[12,13] Namely, the electric potential inside the reflectron is linear, or increases linearly with the distance from the reflectron entrance. Such a design has the advantage that high resolution is maintained for all the ions generated inside the MALDI source, or prompt ions. In tandem mass spectrometry, however, the resolution deteriorates rapidly as the daughter ion mass decreases.[14] Resolution at the low mass region can be improved by lowering the reflectron potential. Hence, the usual strategy is to record tandem mass spectra at several reflectron voltages and to stitch them together to get the full spectrum.[14] An alternative is to use voltage lifting technique which requires a complicated instrumentation.[15]

In our initial attempt to check feasibility of the photodissociation scheme for tandem mass spectrometry, a home-built tandem TOF mass spectrometer equipped with a constant field reflectron was used. Even though efficient photodissociation of protonated peptides was observed, the photofragment signals were difficult to detect due to various complications such as the presence of tremendous background noise. Theoretically, a reflectron with a quadratic potential component in addition to the usual linear one (linear-plus-quadratic, LPQ) can resolve daughter ion signals better. This was designed and installed.[10] With additional efforts to identify and eliminate background noise, decent photofragment spectra could be obtained. At the full acceleration voltage, quality of the tandem mass spectra at the daughter ion masses less than 50% of the precursor mass recorded with this instrument was poor. Even though a full spectrum could be obtained by recording the tandem mass spectra at reduced reflectron potentials and stitching them together, the whole process was inconvenient and inadequate for automation.

The second generation MALDI-TOF-PD-TOF instrument

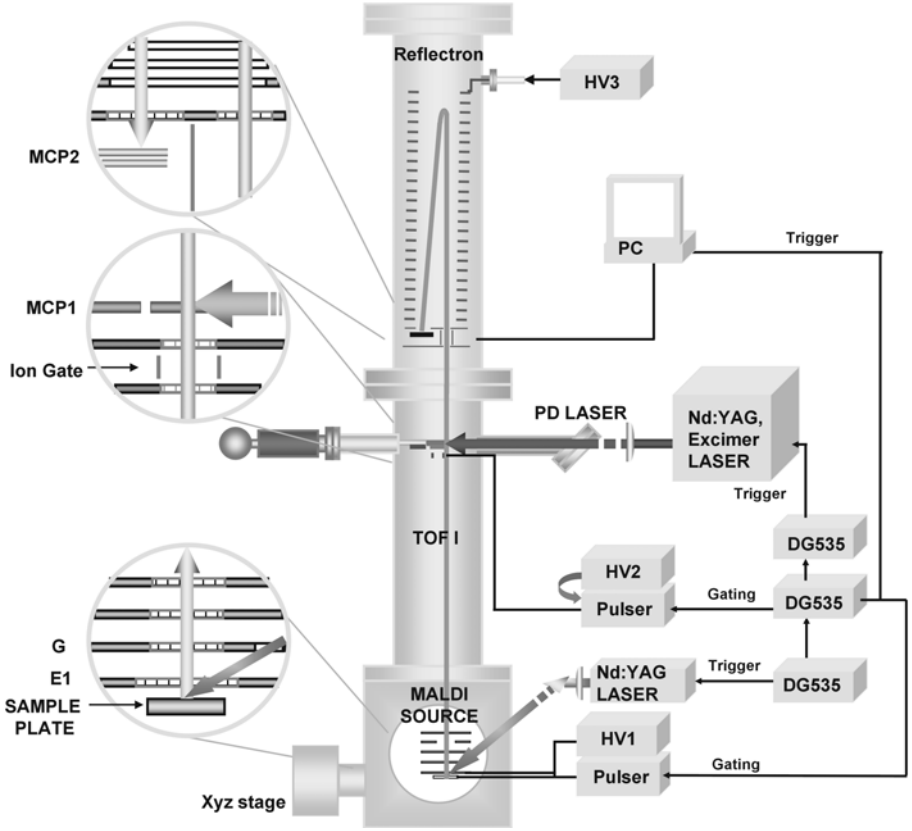

Figure 1. A schematic diagram of the improved MALDI-TOF-PD-TOF instrument built in this work. See text for details.

with an LPQ reflectron designed by utilizing the knowledges gained through operation of the first generation instrument has been constructed. Its important characteristics, both in instrumentation and data system, and performance features are reported in this paper.

Instrumentation

A schematic diagram of the instrument is shown in Figure 1. The instrument consists of a MALDI source with delayed extraction, a flight tube (the first TOF) to time-separate the prompt ions generated by MALDI, an ion gate to select a parent ion, an LPQ reflectron, and a detector. Some features of the present instrument are similar to those of the previous one.[10] Detailed explanations will be made mostly for the features which are different from the previous design. These include the LPQ reflectron and the data system.

A. The first stage mass spectrometer. This part consists of the sample introduction system, the MALDI source with delayed extraction, and the first multichannel plate detector (MCP, 18 mm o.d., Burle, Lancaster, PA). The source was constructed for the maximum acceleration voltage of 30 kV rather than 20 kV in the previous design. A sample plate is introduced via a vacuum lock and mounted on an xyz-translational stage. Movement of the sample plate is completely controlled by a computer. Distance between the ion source and the first time focus is 660 mm. The instrument is operated at 50 Hz rather than at 10 Hz in the previous design. The third harmonic, 355 nm, of a 50 Hz Nd:YAG laser (Powerlite 6050, Continuum, Santa Clara, CA) with 6ns pulse width is used for MALDI. The first MCP on a movable mount is slided into the first time focus when needed.

B. Parent ion selection and photoexcitation. This part is essentially the same as in the previous design.[10] An ion gate with the mass resolving power of 30 is placed just before the first time focus. The fourth harmonic, 266 nm, of another 50 Hz Nd:YAG laser (GCR 150, Spectra-Physics, Mountain View, CA) with 6 ns pulse width or 193 nm output from an excimer laser (PSX-100, MPB Communications INC., Montreal, Quebec) with 2.5 ns pulse width is irradiated perpendicularly to the ion beam direction. The laser pulse is synchronized with the parent ion pulse by using delay generators (DG535, SRS, Sunnyvale, CA).

C. The second stage mass spectrometer. The main component of this stage is the LPQ reflectron. The ion optical principle concerning its performance was described in details previously.[10] A brief outline is as follows.

A reflectron with constant electric field inside, or a linear potential reflectron, can be considered as a lens satisfying the time focusing equation roughly given by

$$L_1 + L_2 = 4d \quad (1)$$

Hence L_1 is the distance of the object, or the first time focus position in the present case, from the reflectron entrance, L_2 is that of the image, or the detector, and d is the penetration

depth of an ion beam. d is essentially the same for all the prompt ions regardless of their masses while it changes with mass for the daughter ions. This is the reason why the resolution gets poorer as the daughter ion mass decreases while it remains virtually the same in ordinary mass spectra, or spectra for the prompt ions. By using a longer (d) reflectron, L_1 can be made longer, and more reaction time can be provided for the photoexcited parent ions.

Perfect time focusing for the daughter ions can be achieved by using a reflectron with quadratic potential inside. However, various difficulties are encountered in using such a reflectron as the second analyzer because both L_1 and L_2 are zero. For example, sufficient time cannot be provided for the dissociation of photoexcited parent ions.

The LPQ reflectron with the inside potential given by the following equation lies halfway between the above two limits.

$$V = c_1x + c_2x_2 \quad (2)$$

Here x is the distance of an inside point from the reflectron entrance. We showed in a previous report[10] that time focusing could be achieved for all the prompt ions using this reflectron. As the quadratic component gets larger, L_1 gets smaller and the daughter ion resolution gets better. Namely, the LPQ reflectron can be thought as a compromise between the linear and quadratic reflectrons. We have found evidences, even though not concrete, in the PD experiments performed with the first generation instrument that the photodissociations observed were occurring rather fast and would not require very long reaction length (L_1). Hence, in the new design, L_1 has been made just as long as needed to accommodate a deflector and the second MCP. Accordingly, a larger quadratic component and a longer reflectron length have been used than in the previous design for better resolution of the daughter ion signals. In the instrument constructed, L_1 is 280 mm and the total length of the reflectron is 530 mm. The reflectron consists of 31 parallel ring electrodes (i.d. = 60 mm, o.d. = 130 mm, thickness = 1 mm) spaced by 16 mm. The optimum values of c_1 and c_2 in eqn. (2) were estimated through ion trajectory calculations using the SIMION[16] package, which were c_1 = 17080 volt·m^{-1} and c_2 = 57740 volt·m^{-2}. Only the final electrode of the reflectron is connected directly to a high voltage power supply. To generate the desired LPQ potential inside, each pair of the neighboring electrodes is connected by a resistor. Resistance values were determined by SIMION calculations also.

In the previous design, an ion beam passed through a center-holed MCP, entered the reflectron, reflected back, and arrived at the MCP. To avoid transmission of the reflected beam through the hole, the reflectron was tilted slightly (0.9°) with respect to the ion optical axis, resulting in deflection of the ion beam. Since the kinetic energy of a daughter ion is proportional to its mass, lower mass ions penetrate the reflectron less and are deflected less. Then, when the instrument is optimized to detect the parent ion,

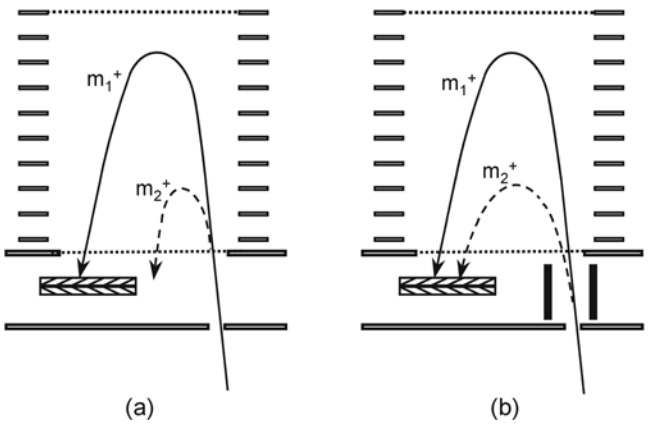

Figure 2. A schematic drawing of ion beam paths in the reflectron (a) without and (b) with deflection before entering the reflectron entrance. m_1^+ is an ion generated in the ion source, or a prompt ion and m_2^+ is a low mass daughter ion.

there is a chance that low mass daughter ions do not hit the detector as shown in Figure 2(a). Through experiments, we found that this was one of the problems in detecting low mass ions together with the parent ion for the previous instrument. Poor resolution and low detector sensitivity for low mass ions were another reasons. In the new design, an MCP (Burle, Lancaster, PA) with large effective diameter, 40mm, is installed off-centered to the reflectron axis. A deflector is installed before the reflectron entrance which deflects ion beam toward the reflectron axis. Since lower mass ions are deflected more by the deflector than the high mass ions, it is possible to guide ions such that ions with widely different masses hit the effective area of the MCP as shown schematically in Figure 2(b). The deflector consists of two parallel electrodes, 40 mm × 70 mm, separated by 20 mm. Typical potential difference applied is 180 V.

D. Data system. The data system serves two purposes, instrument control and data acquisition and processing.

Instrument control: This is achieved by a D/A card (NI-PCI6703, National Instruments, Austin, TX) and a GPIB card (NI-PCIGPIB, National Instruments, Austin, TX). Its functions include mounting of the sample plate in the MALDI source, control of various voltages and delay times for instrument tuning, control of MALDI laser pulsing, ion gate timing control for parent ion selection, and PD laser pulse timing control for laser pulse-ion pulse synchronization. When the parent ion signal is not observed for 50 successive MALDI pulses, the sample plate is moved by 20 um automatically.

Data acquisition and processing: In our previous design, MCP output was sent to a digital storage oscilloscope (DSO). It took 1sec to transfer a spectrum from DSO to the computer while MALDI was running at 10 Hz. To improve the duty factor, average over 10-20 MALDI shots was made in DSO and the result was transferred to the computer. In the new design, an A/D card (CS82G, Gage Applied Technologies, INC., Montreal, Quebec) is used instead of DSO and the spectrum from each MALDI shot is transferred to the

computer. Advantage of this approach is as follows. Since the number of a parent ion in each MALDI shot is only around 100, the number of daughter ions in each time bin of the tandem mass spectrum is usually less than one. Namely, a single shot tandem mass spectrum consists of single ion pulses mostly. Intensities of these single ion pulses can be made larger than the noise level by increasing the MCP gain. Our practice is to adjust the MCP gain such that the single ion pulse height at m/z 100 is larger than the noise level by a factor of 2 or 3. Then, a threshold is chosen at slightly above the noise level. Any signal below this threshold is set to zero. This eliminates various background noises such as the Johnson noise and the rf noise. Elimination of the noises arising from MCP ringing is another advantage of this approach. Setting a clearcut threshold is difficult when averaging is made for 10-20 shots as was done in the previous instrument. After thresholding, each ion pulse is fit to a Gaussian function. This is to minimize noises in ion pulses and to make peak finding easier. The single shot spectra thus processed are averaged over 1000-5000 shots as needed. Mass scales of the MALDI and tandem mass spectra were calibrated using the methods described in ref. 10. The maximum errors in the m/z values were 0.1 and 0.4 amu, respectively.

Experimental Section

Operation. A sample is loaded on a 30 mm × 40 mm stainless steel plate, which is introduced to the source via a homemade vacuum lock and mounted on an xyz- translational stage. The voltage applied on the sample plate and the final electrode of the reflectron are 20 and 25 kV, respectively. To record a MALDI spectrum, an extraction pulse of 1.8 kV is applied to the sample plate some time after the MALDI laser pulsing. Two delay generators are used for this purpose, one for the MALDI laser pulsing and the other for the extraction voltage pulsing. The second delay generator also triggers the A/D card. To record a PSD spectrum, the ion gate is opened when the selected parent ion arrives, which is controlled by the second delay generator. In a PD experiment, the PD laser is triggered such that its pulse arrives at the first time focus in synchronization with the selected parent ion pulse. PD laser pulsing is controlled by another delay generator. When the intensity of the parent ion peak remains very weak for 50 successive runs, the xyz-translational stage is activated to change the sample position as mentioned earlier. A spectrum with a very weak MH^+ peak or with strong but broad MH^+ peak is discarded in data processing.

Samples. Angiotensin II and the matrix, α-cyano-4-hydroxy cinnamic acid (CHCA), were purchased from Sigma (St. Louis, MO) and used without further purification. Matrix solution was prepared daily using acetonitrile and 0.1% trifluoroacetic acid, which was mixed with the peptide solution. The final peptide concentration prepared for the PD experiments was ~10 pmol/μL. 1 μL of the solution was loaded on the sample plate.

Results and Discussion

The MALDI spectrum of angiotensin II recorded by the new instrument is shown in Figure 3. The resolving power of the spectrometer estimated from the full width at the half maximum of the protonated peptide peak, MH^+, is around 8000, better than 5000 observed with the previous instrument. Higher acceleration voltage used is one of the reasons for better resolution. The second MCP installed in the new instrument has smaller channel diameter than the previous one, 10 um vs. 25 um, and has been found to result in better resolution.[17] Small peaks at 1047.1, 1047.3, and 1048.1 are artifacts due to MCP ringing.

The PSD spectra of the protonated angiotensin II are shown in Figure 4. The spectrum (a) is the raw data averaged over 3000 MALDI shots. The broad AC background is due

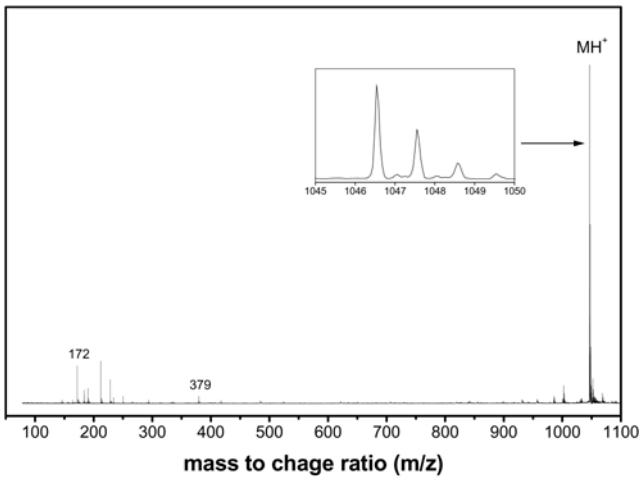

Figure 3. MALDI spectrum of angiotensin II averaged over 100 laser shots. The peak width of MH^+ is 3 ns. Small peaks at m/z 1047.1, 1047.3, and 1048.1 are due to MCP ringing.

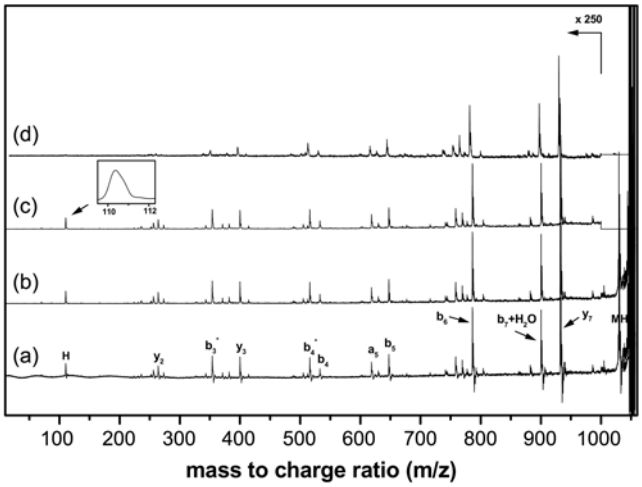

Figure 4. PSD spectrum of MH^+ from angiotensin II. (a) is the average of the raw single shot spectra, (b) is the average of the thresholded spectra, and (c) is the average of the Gaussian-fit spectra obtained with present instrument. (d) is the average of the raw spectra obtained with the previous instrument.

the AC noise present in the A/D card. Also to be noted is the presence of the negative and positive peaks accompanying each peak, which are due to MCP ringing. Even though these are prominent features in the averaged spectrum, they are weaker than single ion pulse heights in a single shot spectrum. Hence, these can be removed readily by setting a proper threshold as described in a previous section. Averaging the thresholded spectra resulted in a dramatically improved spectrum as shown in Figure 4(b). Finally, each single shot spectrum was treated with Gaussian fitting and summed. The result is shown in Figure 4(c). Even though the improvement achieved here does not look as impressive as that made in the previous step, it helped tremendously in finding peaks automatically by the data system. The same spectrum obtained with the previous instrument at its full acceleration voltage is shown in Figure 4(d). It is to be noted that both the intensities and the resolutions deteriorate rapidly as the daughter ion mass decreases in this spectrum. Peaks at m/z below 500 are hardly useful for structure determination, which was the reason why recording at lower reflectron voltages was needed with the previous instrument. In contrast, low mass peaks can be identified in the spectra obtained with the present instrument, as demonstrated in the inset in Figure 4(c). The bandwidth of the peak at m/z 110 in the inset is 0.8 amu, showing that unit mass resolution has been achieved even at 10% of the parent ion mass. Namely, recording the tandem mass spectra at several reflectron voltages and stitching them together are not needed with the present instrument. Instrument control and data handling needed to assure reliable stitching, which are rather complicated, time-consuming, and sometimes erroneous, can be avoided. Also to be noted is that the noise level in Figure 4(c) is lower than that in Figure 4(d). This helps in peak finding and mass calibration.

As has been explained already, the photo-induced spectral change in a tandem mass spectrum, or the PD spectrum, is obtained by subtracting the PD laser-off (PSD) spectrum from the PD laser-on spectrum. The PD spectrum of the protonated angiotensin II obtained at 193 nm is shown in Figure 5(a). Some signals in this spectrum appear as the negative signals. These are mostly due to photodissociation of the fragment ions generated by PSD of the parent ion which arrive at the irradiation region at the same time. The same spectrum obtained with the previous instrument at its full acceleration voltage is shown in Figure 5(b) for comparison. A dramatic improvement in spectral quality achieved with the present instrument is obvious. Also to be mentioned is that the total experimental time needed to obtain the spectrum with the present instrument is only a few percent of that needed with the previous instrument.

Two further characteristics of the PD spectrum in Figure 5(a) are to be discussed. One is the fact that the widths of PD peaks are narrower than those of PSD peaks at similar m/z. For example, widths of the peaks at m/z around 100 in Figure 5(a) are 0.5 amu which is narrower than 0.8 amu observed at the same m/z range in the PSD spectrum. An explanation is as follows. Daughter ions diverge spatially due to the kinetic energy release in the dissociation step, which disturbs the beam quality and results in deterioration of the resolution. In PSD, daughter ions generated over the entire field-free region between the ion source exit and the reflectron entrance are detected. The beam quality must be poorer for daughter ions generated near the source than those generated near the reflectron. In contrast, the daughter ions in the PD spectrum are those generated between the first time focus and the reflectron entrance. Hence, deterioration of the beam quality is less in PD, resulting in slightly better resolution than in PSD.

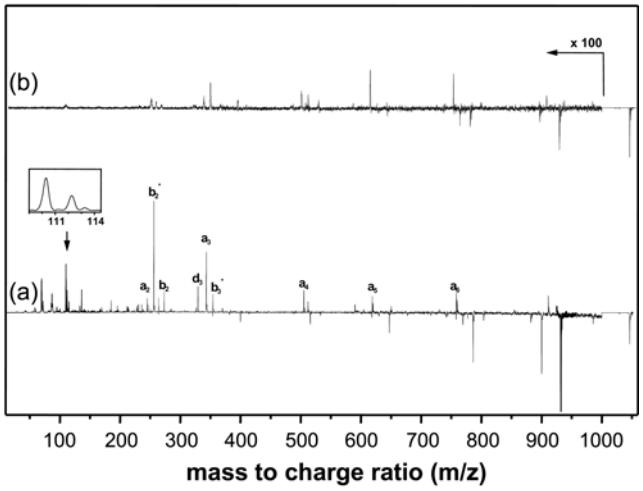

Figure 5. PD spectra of MH^+ from angiotensin II obtained (a) with the present instrument and (b) with the previous instrument at the full acceleration voltage of each instrument.

The other feature is that the background level in the PD spectrum, Figure 5(a), decreases slightly as m/z increases. Recalling that the PD spectrum is obtained by subtracting the PSD spectrum from the laser-on spectrum, the above means that the background level at high m/z of the laser-on spectrum is lower than in the PSD spectrum. It is well known that the rate constant for dissociation of a parent ion increases as its internal energy increases.[18] On the average, some of the parent ions with the internal energy a little less than those dissociating before the reflectron will dissociate during the flight inside the reflectron. Daughter ions formed inside the reflectron do not form regular peaks in the tandem mass spectra but appear as a broad structureless tail in the short flight time side, or low mass side, of the parent ion peak. Single ion pulses which do not form peaks after averaging are called chemical noises. Ions generated inside the field, such as in the reflectron, are the major source of chemical noise in well-designed mass spectrometers. Then, the fact that chemical noise is less in PD than in PSD means that dissociation inside the reflectron occurs less frequently after photoexcitation. Or, photodissociation occurs mostly before entering the reflectron or occurs rather fast. This is the indirect evidence mentioned earlier which led to the present design of the second stage analyzer with a short distance between the first time focus and the reflectron entrance. It is to be emphasized that construction of a

tandem PD-TOF mass spectrometer with better than unit mass resolution in low m/z range would not have been possible if sufficient photodissociation time had been provided as in the previous instrument.

Even though the present instrument is a great improvement over the previous one, there are areas in which further improvements are needed. One of these is in monoisotopomeric selection of a parent ion when the resolution of the first stage analyzer is not sufficient for the purpose such as in the cases of high mass parent ions. Investigation is under progress to handle this problem either by further improving the instrument or by improving the data system.

Acknowledgments. This work was financially supported by CRI, Ministry of Science and Technology, Republic of Korea. Postdoctoral fellowship to J. H. Moon was supported by CRI. S. H. Yoon thanks the Ministry of Education for the Brain Korea 21 fellowship.

References

1. Tanaka, K.; Waki, H.; Ido, Y.; Akita, S.; Yoshida, Y.; Yoshida, T. *Rapid Commun. Mass Spectrom.* **1988**, *2*, 151.
2. Karas, M.; Bachmann, D.; Bahr, U.; Hillenkamp, F. *Int. J. Mass Spectrom. Ion Processes* **1987**, *78*, 53.
3. Kaufmann, R.; Kirsch, D.; Spengler, B. *Int. J. Mass Spectrom. Ion Processes* **1994**, *131*, 355.
4. Franzen, J.; Frey, R.; Holle, A.; Kräuter, K. O. *Int. J. Mass Spectrom.* **2001**, *206*, 275.
5. Hettick, J. M.; McCurdy, D. L.; Barbacci, D. C.; Ruessell, D. H. *Anal. Chem.* **2001**, *73*, 5378.
6. Guan, Z.; Kelleher, N. L.; O'Connor, P. B.; Aaserud, D. J.; Little, D. P.; McLafferty, F. W. *Int. J. Mass Spectrom. Ion Processes* **1996**, *157/158*, 357.
7. Preisler, J.; Yeung, E. S. *Anal. Chem.* **1997**, *69*, 4390.
8. Thompson, M. S.; Cui, W.; Reilly, J. P. *Angew. Chem. Int. Ed.* **2004**, *43*, 4791.
9. Park, S. T.; Kim, S. K.; Kim, M. S. *Nature* **2002**, *415*, 306-308.
10. Oh, J. Y.; Moon, J. H.; Kim, M. S. *J. Am. Soc. Mass Spectrom.* **2004**, *15*, 1248-1259.
11. Oh, J. Y.; Moon, J. H.; Kim, M. S. *Rapid Commun. Mass Spctrom.* **2004**, *18*, 2706-2712.
12. Mamyrin, B. A.; Karataev, V. I.; Shmik, D. V.; Zagulin, V. A. *Sov. Phys. JETP* **1973**, *37*, 45-48.
13. Rockwood, A. L. *34th Annual Conference on Mass Spectrometry and Allied Topics*; Cincinnati, OH, 1986.
14. Medzihradszky, K. F.; Campbell, J. M.; Baldwin, M. A.; Falick, A. M.; Juhasz, P.; Vestal, M. L.; Burlingame, A. L. *Anal. Chem.* **2000**, *72*, 552.
15. Cotter, R. J. *Time-of-Flight Mass Spectrometry*; ACS: Washington, U. S. A., 1997; p 47.
16. Dahl, D. A. *SIMION 3D version 7.0*; Idaho Falls, ID, 2000.
17. Vestal, M.; Juhasz, P. *J. Am. Soc. Mass Spectrom.* **1998**, *9*, 892.
18. (a) Robinson, P. J.; Holbrook, K. A. *Unimolecular Reactions*; Wiley-Interscience: New York, 1972; pp 1-108; (b) Forst, W. *Theory of Unimolecular Reactions*; Aacademic Press: New York, 1973; pp 3-70.